POTENTIAL BENEFITS OF INTEGRALLY STIFFENED AIRCRAFT STRUCTURES

L. U. Hansen, S. M. Häusler, P. Horst
Institute of Aircraft Design and Lightweight Structures (IFL), TU Braunschweig
Hermann-Blenk-Str. 35, D- 38108 Braunschweig
Germany

ABSTRACT

Integrally stiffened structures are of considerable interest due to innovative manufacturing methods. On the one hand they offer the possibility to use completely new topologies, but on the other hand they lack certain abilities in damage tolerance. In this paper both sides are considered: An optimization scheme and some results are presented that make use of the freedom of design obtained by new manufacturing methods. The consideration of crack growth in integral structures and the associated challenges are discussed.

The definition of dimensions and the choice of an ideal topology define the optimization task that is solved by the application of an optimization procedure based on an Evolution Strategy. Constraints are defined by damage tolerance and stability criteria. Exemplarily the window area of a generic aircraft fuselage, utilizing an innovative integral design, is idealized by finite elements and investigated with regard to three load cases that consider linear and nonlinear solutions. Multiple design responses, including a response based on crack extension, form a single fitness function and define the design objective. The basis for the optimization is provided by a parametric finite element model that covers a variety of changes to the topology and shapes of stiffeners and frames. A parallel evaluation of the structural responses decreases computing time.

The consideration of damage tolerance behavior of integral structures requires special attention by crack growth calculations and is covered in this work using a method based on a crack closure technique. It is proved that this simple method is capable of calculating relatively complex crack scenarios but fails when it comes to crack extension into the stiffeners. Obviously more sophisticated methods are required to cover such aspects. The 6th FP project DaToN of the European Commission [6] that aims to address these scenarios is presented.

1. INTRODUCTION

The strong impact of structural weight on fuel efficiency and aircraft performance motivates improvements of today's structural airframe design. Besides changes in the material (e.g. carbon fiber laminates) another design alternative might be provided by topological changes of integrally stiffened, metal structures. They could offer weight improvements (relative to conventional built-up design weights) and reduce material and manufacturing costs (compared to costs for composite structures).

The conventional metal fuselage design has remained almost unchanged over decades although new manufacturing techniques have been developed that allow for significantly different designs. The increased freedom of design which is offered by techniques like High Performance Cutting (HPC), Laser Beam Welding (LBW) and Friction Stir Welding (FSW), enables the employment of topologies that are not rectangular and that correspond to the occurring loads more efficiently.

Despite these possible advantages a main drawback is the poor damage tolerance behavior of integral structures since cracks can propagate into the stiffening members of the structure and eventually cut them. A second load path, like in differential structures, is not available. Consequently all design evaluations need to pay special attention to this effect. [6] While previous investigations of integrally stiffened structures often paid attention to manufacturing aspects, as in [9] and [12], this paper focuses on the fatigue crack and stability assessment of such structures.

A design example of an integrally stiffened structural concept for a transport aircraft, based on solutions shown by [5], [6] and [11] is presented in this paper. The application of integral structures for the highly disturbed window area of a fuselage structure is investigated. With respect to damage tolerance and stability criteria a minimum weight solution is sought. The large design space, realizable due to innovative manufacturing methods, can be explored by using an Evolutionary Algorithm. The objective and constraints are evaluated by linear and nonlinear simulations with finite element models of the structure. One crack scenario is considered for the investigation of the crack growth by means of the Virtual Crack Closure Technique.

This paper is structured as follows: Section 2 gives an introduction in the challenges of integrally stiffened structures and introduces the methods used for their design assessment. In section 3 the investigation of a window belt area and its optimization approach is presented. The results of the optimization are shown in section 4. In section 5 the aim of the project DaToN is defined and in section 6 a conclusion is given.

2. DESIGN CHALLENGES OF INTEGRALLY STIFFENED STRUCTURAL CONCEPTS

Different design objectives and design requirements have to be considered during the investigation of integral structures. Depending on the design objective under investigation two different groups can be outlined:

- Manufacturing aspects: Objective of minimizing manufacturing time and costs with respect to constraints defined by manufacturability.

- Structural and mechanical aspects: Objective of minimizing weight w.r.t. compliance, stability, fatigue and strength criteria.

The representation of the manufacturing aspects in numerical simulations bears problems due to the difficulty in expressing the ease of manufacturing unless a good cost estimate is available. In order to cope with this situation a different approach has been chosen. A parametric model of an integral structure is used which only creates topologies that can be manufactured. Changes in the size of the members, e.g. stiffener heights, are controlled by spline functions and consequently do not show unsteady and undesired transitions. In addition, pre-defined ranges of parameters are used to limit the design space to models that comply with manufacturing requirements.

The required investigation and optimization is hence reduced to a problem defined by structural / mechanical aspects. Nevertheless a final review of the manufacturing constraints is suggestive.

The investigation of the structural and mechanical behavior of the structure needs to pay special attention to the relevant criteria in order to be able to compare the results (as well in comparison with a differential reference structure). A limited number of characteristic load cases and corresponding criteria are chosen to cover multiple criteria during the investigation. These criteria, including fatigue cracking, residual strength and stability, are presented in the subsequent sections.

2.1. Fatigue

2.1.1. Virtual Crack Closure Technique

The stress intensity factors are calculated by means of a crack closure technique. This technique is based on the assumption that the energy released when extending a crack is equal to the energy required to close the crack. The calculation of the forces and displacements near the crack tip is sufficient to evaluate the stress intensity factors without the need to introduce significant changes to the finite element model. Solely elements need to be separated in order to establish a cracked condition. The displacements and the forces of a pair of nodes close to the crack tip are used to calculate the work required to establish the uncracked, original position. These forces correspond to the forces acting on the upper and lower surface of the closed crack. The differences between the cracked and uncracked states need to be investigated in two analyses: the forces at the closed crack and the forces and displacements at the open crack have to be determined in consecutive linear analyses.

Further simplification is achieved by a so-called virtual crack closure technique (VCCT) that introduces an additional assumption: the crack extension of a small Δa does not change the state close to the crack tip significantly. This allows for a one-step evaluation by using results of just one linear analysis. The required energy release rate G, necessary for a virtual extension of the crack, is assumed to create the same crack opening displacement as for the unextended crack [8]. FIG 1 depicts an exemplary crack length for a damage scenario of an edge crack. The necessary parameters for evaluation, such as the displacements and forces, are given in the figure.

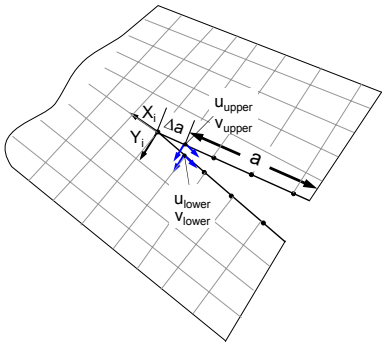

FIG 1. crack tip model for application of the VCCT (for clarity the forces at the crack tip are shown for one side of the crack only)

If the nodes at the crack tip are nearly equidistant and four-node shell elements are used, the energy release rate is defined by the following two relations [8]:

(1) $$G_I = -Y_i \cdot \frac{\left(v_{lower} - v_{upper}\right)}{2 \cdot \Delta a \cdot t}$$

(2) $$G_{II} = -X_i \cdot \frac{\left(u_{lower} - u_{upper}\right)}{2 \cdot \Delta a \cdot t}$$

with

a	crack length
t	thickness
G_I	energy release rate, mode I crack
G_{II}	energy release rate, mode II crack
u	displacements in crack direction
v	displacements normal to the crack surface
X_i	nodal force at the crack tip in growth direction, upper or lower crack surface node
Y_i	nodal force at the crack tip normal to growth direction, upper or lower crack surface node
upper	Index for upper crack surface
lower	Index for lower crack surface

Under the assumption of linear elastic fracture mechanics and a plane stress state, the energy release rates can be related directly to the stress intensity factors K_I and K_{II}

(3) $$K_I = \sqrt{G_I \cdot E}$$

(4) $$K_{II} = \sqrt{G_{II} \cdot E}\ .$$

For simplification, only the mode I stress intensity factor K_I will be regarded for succeeding crack growth calculations, while K_{II} and K_{III} are not considered. The number of load cycles required to grow the crack from an initial to a maximum crack length, is taken as a mean to rate the fatigue behavior (comparable to an inspection interval). Due to the limitation to plane problems, the VCCT cannot be applied to study the crack extending into the stiffening members. Consequently the maximum crack length that can be evaluated, is defined as the length of the crack when it reaches the (integral) stiffener.

2.1.2. Crack growth

Crack growth life can be investigated under the assumption that the number of load cycles required to extend a crack can be based on stress intensity factors (SIF) calculated for several discrete crack lengths. A functional rela-

tion between crack length and SIF is created by a least square fit using a polynomial function (here a polynomial of degree 2 has been chosen). It is obvious that the SIF for short crack lengths and for long crack lengths are of significant importance to fit the spline and to estimate the crack growth rates correctly.

The crack growth rate is calculated by Forman's equation [7]:

(5) $$\Delta K \le \Delta K_{th}: \quad \frac{da}{dN} = 0$$

(6) $$\Delta K > \Delta K_{th}: \quad \frac{da}{dN} = \frac{C_f \cdot (\Delta K)^{n_f}}{(1-R)\cdot K_C - \Delta K}$$

(7) $$\frac{\Delta K}{(1-R)} \ge \cdot K_C: \quad \frac{da}{dN} = \infty$$

The required load cycles for defined crack propagation are determined by integration of eq.(6):

(8) $$N(a) = \int_{a_1}^{a_2} \frac{(1-R)\cdot K_C - \Delta K}{C_f \cdot (\Delta K)^{n_f}} da$$

with

K	stress intensity factor (SIF)
N	number of load cycles
R	load ratio
A, B, k, C_f, n_f, K_c	material properties
ΔK_{th}	threshold value ($= A \cdot (1 - B \cdot R)^k$)

2.2. Residual strength

The residual strength criterion is based on an ultimate load case. The fuselage structure is pressurized with maximum differential pressure, typically 2Δp, and required to withstand these loads even with a certain initial damage.

A damage scenario with a crack reaching the adjacent frame is considered as a critical case. The criterion for instable crack growth (eq. (7)) is applied to verify if the structure can withstand the ultimate load.

2.3. Stability (Nonlinear Stability Model)

A fundamental criterion for fuselage structures is the stability and buckling performance. In this context global buckling behavior seems to be the appropriate stability criterion, since local buckling is not necessarily limiting today.

The innovative and probably non-rectangular stiffener topology requires a higher effort for the assessment of this point. Analytical methods for non-rectangular fields are not at hand or only applicable to certain arrangements. Methods to investigate the global buckling limits, such as the determination of effective widths, are not available.

Therefore another approach is used: the stability is judged by investigation of the displacement of certain nodes along a path through the structure. Subjected to ultimate load level the radial deformation determined by a non-linear finite element analysis is taken as a measure for the global buckling behavior. A specific implementation of this criterion is shown in section 3.7.5.2.

3. INTEGRALLY STIFFENED STRUCTURAL CONCEPT

3.1. Introduction

The application of integral structures in the highly disturbed window area of a fuselage structure is of special interest. Today's metal fuselage design is in principle composed of skin, frames and stringers. The windows are generally located between two frames and feature a fairly high window frame. This area experiences a very disturbed loading condition with special challenges due to the stress concentrations at the window corners.

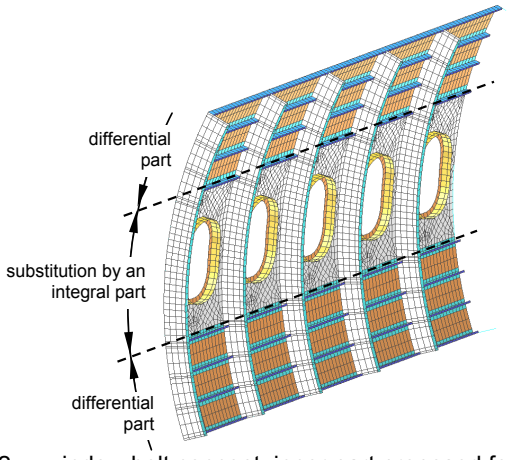

FIG 2. window belt concept: inner part proposed for substitution by an integrally stiffened structure

The adaptation of the stiffener topology to the local loading situation has potential to improve the structure's performance. Typically the fuselage structural loading is dominated by fuselage bending loads and recurring pressurization loads. Consequentially a pure compliance-driven optimization, even under consideration of critical buckling loads, does not adequately represent the real requirements for such a structure.

The presented approach hence covers the recurring limit loads by means of a fatigue crack investigation, ultimate fuselage bending loads by a nonlinear stability analysis and residual strength at 2Δp pressurization.

3.2. Geometry

The models under investigation represent a window area of a short range, single aisle fuselage structure of a conventional aircraft. The models feature a fuselage radius of 1975 mm, a frame pitch of 520 mm and a length of 2600 mm. The lower edge of the model is defined by the passenger floor of the aircraft. The (vertical) height of the model is approximately 1450 mm. To simplify the geometry a symmetric arrangement with three stringers below and above the windows is chosen.

The area subjected to optimization (as described in section 3.7) is limited to the window belt. This area is proposed to be substituted by an innovative, integral part (as shown in FIG 2 and FIG 3). The integrally stiffened window belt is machined from solid metal via High Performance Cutting (HPC). The surrounding structure is a conventional, built-up structure. The differential and integral part are joined by welding techniques (Laser Beam Welding,

Friction Stir Welding) or by a riveted lap joint.

An integral window part, created by HPC, has been shown by Pacchione [11] in 2006. It is obvious that the size of the semi-finished part and the chipping ratio is directly related to the desired stiffener and window frame height. As a consequence the maximum allowable stiffener height is limited during the design optimization.

Due to the investigation of two different window panels (located in the forward and aft fuselage) the geometry of the basis structure is slightly different for each panel.

Location	h_{frame} /(mm)	$b_{frame\ flange}$ /(mm)	$t_{frame\ flange}$ /(mm)	$t_{frame\ web}$ /(mm)	t_{skin} /(mm)
Forward	110 mm	24 mm	3 mm	2.5 mm	2 mm
Aft	80 mm	15 mm	2 mm	2 mm	2 mm

TAB 1. location and dimensions of panels

The frame dimensions, the skin thickness (as shown in TAB 1) and the Z-shaped stringers of the differential part (height h_s = *25 mm*, head width b_{hw} = *8 mm*, foot width b_{fw} = *25 mm*, thickness t_s = *2.0 mm*, foot thickness t_{fs} = *2.5 mm*) remained constant during each design investigation.

The skin thicknesses were defined with 2 mm (TAB 1). The window size was set to a size of 193 mm x 150 mm and a corner radius of 135 mm. The window rest remained constant with a width of 22 mm and a thickness of 6 mm. The window frame thickness was 4.5 mm. All differential versions feature a window frame height of 30 mm.

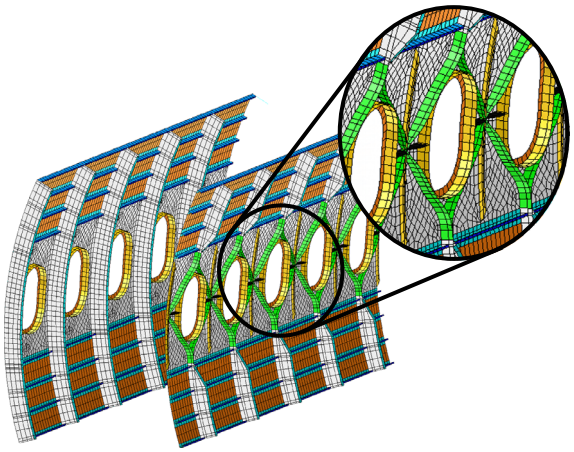

FIG 3. conventional and innovative fuselage structure

The finite element models were composed of 2D shell elements (MD Nastran® CQUAD4) with bi-linear shape functions that feature a good compromise of numerical efficiency and accuracy in linear and nonlinear solutions.

Two principle structural layouts were under investigation (as shown in FIG 3): a conventional structure and an alternative, innovative structure. The innovative structural design exhibits a different stiffener topology and a different location of the window. Similar to an in-house design idea, as presented by [11], the window is positioned in the frame, creating a “joint window frame” design (*JWF*-design, [5]). The combination of window frame and (fuselage) frame reduces in total the required frame material. In order to improve the fatigue and the stability behavior additional stiffeners are integrated in the window belt area.

3.3. Material

For simplicity a single material was chosen for the complete structure[1] with the following properties: Young’s modulus E = *71700 MPa*, Poisson’s ratio ν = *0.3* and density ρ = *2800 kg/m³*. The Forman coefficients were taken from [7]: A = *87*, B = *1*, k = *1*, C_f = *3.39 x 10⁻⁷*, n_f = *2.32* and K_c = *2473 Nmm^3/2* (abbreviations as used in section 2.1.2).

3.4. Loads and Boundary Conditions

Three different load cases were considered: a fatigue load case, a residual strength load case at maximum pressurization and an ultimate bending load case[2].

The loads were determined using a global finite element model based on the capabilities of the in-house tool PrADO (Preliminary Aircraft Design and Optimization Tool). Detailed information on the global finite element discretization and the calculation of loads is given in [3],[4], [5] and especially in [10].

The aircraft’s mass distribution, the aerodynamic properties and loads required to calculate the (static) component loads were based on a recalculation of an Airbus A320 with PrADO. The resulting nodal displacements and rotations along the edges of the panel were extracted from global finite element models for the above mentioned load cases.

Due to the much coarser mesh of the global model the displacements were applied to the local model at certain discrete points only. As a consequence these boundary conditions introduce disturbances that have been reduced by the creation of artificially stiff beams on the outer edges of the local model.

	Criterion	j /(-)	n /(-)	dp /(mbar)	V /(-)	m_{total} /(ton)	loads origin
1	Fatigue	1	1	1Δp = 615	Ma 0.78	68.2	PrADO global FEM
2	Stability	1.5	2.78	0	Ma 0.52	62.0	
3	Residual Strength	-	-	2Δp = 1230	-	-	-

TAB 2. load cases

Two locations within the fuselage (forward and aft position) were considered in separate optimization tasks to investigate the influence of the panel position (by consideration of the changes in loading conditions) on the optimized design (see. Appendix, FIG 8, FIG 9).

The following load cases were considered:

- A recurring load case based on cabin pressurization, inertia and aerodynamic loads in trimmed, static flight condition (j = 1, 1g, 1Δp).

[1] The validity of the properties is limited to sheet metal. Due to the lack of information the same material properties have been applied as well to the solid material of the machined integral designs.

[2] This selection of loading conditions is made to provide reasonable loads for a first assessment. It is likely that additional cases are required for further investigations.

- An ultimate load case based on maneuver loads with (j=1.5, 2.78g, 0Δp) without cabin pressurization.
- A 2Δp load case solely pressurized without additional flight loads.

3.5. Reference Structures

3.5.1. Differential Reference

As a reference a typical, conventional built-up structure has been created where frames and windows are separate parts. The overall dimensions are given in section 3.2.

The weight of the differential reference, the number of load cycles until maximum crack extension (load case 1, section 2.1, crack scenario described in section 3.7.5.3), the maximum displacement (load case 2, section 2.3) and the stress intensity factor for ~90% crack length (load case 3, section 2.2, crack scenario described in section 3.7.5.3) are summarized in TAB 3 for both investigated sections.

Location	mass /(kg)	N (a_{max}) /(cycles)	d_{max_disp} /(mm)	$d_{similarity}$ /(mm)	$K_{res\ strength}$ /(Nmm$^{3/2}$)
Forward	35.47	30190	1.50	9.93	1521
Aft	32.31	7860	0.85	3.65	1997

TAB 3. performance of *reference* differential structures

3.5.2. Integral Initial Starting Point

In order to define a starting point for the following optimization, an integral structure without any additional stiffeners (as shown in FIG 6) and with a window frame height of 60 mm has been created. The following table gives an overview on the performance of the *initial* integral structures (loads and crack scenarios are identical to the description in section 3.5.1).

Compared with the differential reference structures the initial integral structures are heavier and less stiff. The fatigue behavior is similar but the residual strength criterion is not fulfilled and indicates failure at 2Δp load.

Location	mass /(kg)	N (a_{max}) /(cycles)	d_{max_disp} /(mm)	$d_{similarity}$ /(mm)	$K_{res\ strength}$ /(Nmm$^{3/2}$)
Forward	36.02	48290	3.59	25.24	2497
Aft	34.35	7500	2.00	9.36	2675

TAB 4. performance of *initial* integral structures

3.5.3. Optimization Approach

The optimization is defined by the search for *n* design variables

$$X = [x_i] \quad i = 1,2,...n \tag{9}$$

that minimize the objective function *F* with respect to n_g inequality constraints *g*,

$$g_j(X) \le 0 \quad j = 1,2,...n_g \tag{10}$$

and n_h equality constraints *h*,

$$h_k(X) = 0 \quad k = 1,2,...n_h . \tag{11}$$

Here the objective of the optimization task is to find a structure with a minimum weight which fulfills design requirements and constraints (defined as inequality constraints). The scope of the design space covers different model topologies and topographies, each one composed of parts in different dimensions.

Consequently the representation of such structural layouts requires:

- Design variables that describe the model topology and topography (e.g. existence of additional stiffeners, location of spline control points).
- Design variables that influence the model proportions and, by changing the stiffness distribution, the force flow in the structure (e.g. thicknesses, cross-sectional areas).

3.6. Evolution Strategy

Optimization methods based on Evolutionary Algorithms (EA) simulate Darwin's theory of evolution of the “survival of the fittest”. Multiple generations are investigated until the fitness of the population has significantly improved.

Every individual in the population is defined by a set of design variables (like genes in the genotype of an individual). In order to improve a selection pressure is required that can either be exerted by sorting out the individuals with the lowest fitness or by selecting only the best performing individuals for recombination.

Two different branches of Evolutionary Algorithms have been developed. The Evolution Strategies (ES) and Genetic Algorithms (GA) are based on the same principles but feature different ways to encode the design variables and to impose the selection pressure.

As mentioned, the optimization process requires parameters that describe the model and that characterize each *individual*. These parameters are coded in *genes* that describe each individual's behavior. In the case of the *GA* these genes are represented by binary encodings of the parameters and represent the genotype. A mapping function translates the genotype to the phenotype (e.g. real-value model parameters). In ES the genotype is normally equal to the phenotype which means that every real-valued parameter of the optimization model can be, without mapping functions, part of the genome. In addition to the object variables each individual possesses in ES additional strategy parameters, defining the standard deviations (variances and covariances). The object variables and the strategy parameters are changed by mutation and recombination and are hence part of the optimization problem.

All EA possess certain and specific ways to *recombine*, *mutate* and *select* individuals in order to simulate multiple generations of evolution. Due to the various differences in the EA, this paper deals only with one implementation of an ES with a so-called μ,κ,λ-strategy where the parameter μ denotes the size of the parent population, λ the number of offspring and κ the lifespan of an individual. Depending on the choice of κ this representation includes the $\mu+\lambda$ and μ,λ strategy (comprehensive overviews are given in [1], [13]): The μ,κ,λ - ES includes the lifespan for the survival of the parents as an additional parameter. This allows the selection mechanisms to differ in the *selection pressure*

exerted on the population. Depending on the problem type, different arguments for the choice of an adequate life span can be given (see [5]).

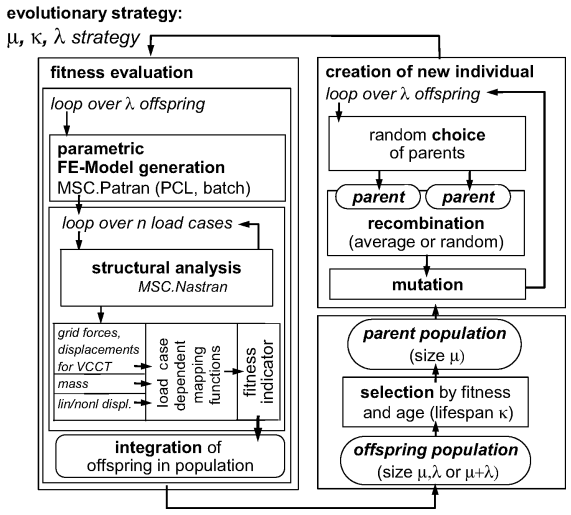

FIG 4. General setup of an Evolution Strategy with external fitness evaluation (model generation: MSC.Patran® PCL, FEA: MD Nastran® 2006)

The principal operations of an ES are, as shown in FIG 4, performed in multiple steps:

- Definition and creation of an initial population with μ individuals
- Creation of λ offspring
  - Random selection of parents out of an initial population
  - Recombination and mutation to create a new individual (offspring)
  - Evaluation of individual's fitness (e.g. FEM based structural analysis, experiment)
  - Integration of individual in population
- Reduction of the population size by age (life span κ)
- Selection of the μ fittest individuals
- convergence check (either restart in step 2 or stop)

The fitness of an individual is the measure for its quality. Depending on the optimization setup the fitness function can contain the objective and the constraints of the system. Different approaches are known on how to include violations of design constraints. The aim is to punish intermediate violations less but without relieving the selection pressure too much (distinction between full and little violation).

3.7. Optimization Setup

3.7.1. Parametric Model

The simulation presented in this paper is based on finite element models. These models are created with the commercial pre- and postprocessor MSC.Patran® by a routine written in PCL (Patran Command Language). To increase the model generation speed, MSC.Patran® has been run in command line mode (batch mode). In this case the parameters are provided by an ASCII-file input; suppressed graphics processing helps to increase the model generation speed.

3.7.2. FE-Model

The finite element models created in MSC.Patran® are translated to MD Nastran® format. Depending on the optimization task different MD Nastran solution sequences are chosen (SOL 101 for linear and SOL 106 for nonlinear analyses).

3.7.3. Evolution Strategy: *EStruct*

The Evolution Strategy used for this investigation is the in-house tool *EStruct* that is written in Python and based on methods proposed by [14]. The routine makes use of the object orientated features of Python by handling each offspring as a separate object of a common class. This basic idea leads to a transparent code that is easy to adapt. The current version features possibilities to restart from an earlier run, to distribute the jobs on multiple machines (nodes) and to calculate the finesses externally (e.g. Ansys, Nastran). The main procedure is described in [5].

3.7.4. Design Variables (DV)

The design variables are used to influence the topology and the dimensions. The first three design variables (discrete variables) are used to control the existence of additional stiffeners:

- 1st DV: vertical stiffener between the windows
- 2nd DV: diagonal stiffener between the windows
- 3rd DV: horizontal stiffener between the windows

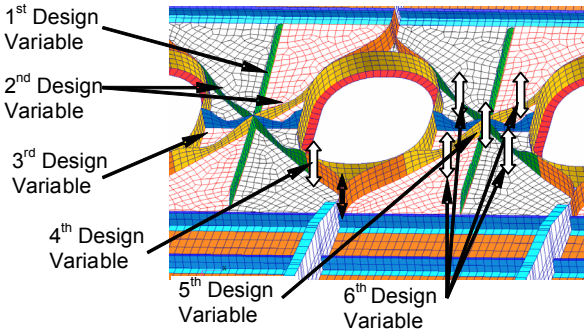

FIG 5. design variables for optimization of integrally stiffened *JWF*-design

The 4th to 6th design variables control the height of the stiffeners by changing the position of spline control points (continuous variables):

- 4th DV: window frame height
- 5th DV: center spline control point
- 6th DV: intermediate spline control point

In order to limit the design space to a reasonable size (e.g. to limit the size of the solid metal before HSC) the following side constraints (SC) have been included;

- 1st SC: 30 mm < $h_{\text{window frame}}$ < 60 mm,
- 2nd SC: 10 mm < $h_{\text{central control point}}$ < 60 mm,
- 3rd SC: 10 mm < $h_{\text{intermed. control point}}$ < 60 mm.

3.7.5. Design Constraints

The design constraints have been included in the objective function by using mapping relations (cp. [2] and [5]). Each structural response ($i = 1,2,\ldots n_{responses}$) is translated

through a transfer function (in the following called mapping function) to a design response *d* which is then included as an addend in the objective (fitness) function *F*:

$$F(X) = \sum_{i=1}^{n_{responses}} w_i \cdot d_i \quad (12)$$

An additional weight factor *w* is used to adjust the impact of each response on the global objective. Within this work *w* has been set to 1.0. In all presented cases the mapping function translates the physical response to an abstract design response *d*. A design response of *d = 0* corresponds to the desired condition and *d > 0* to the undesired condition. Depending on the treatment of intermediate results different functions are suitable:

- Exponential functions allow the design response *d* to increase boundlessly (response of *d > 1.0* possible).
- Step functions or smoothed step-functions restrict the design response between 0 and 1.0 (*0 < d < 1.0*).

3.7.5.1. Mass constraint

The mass mapping function assigns a structural mass to an artificial design response. In order to avoid poor results a desired range of structural masses has been assigned. All structural masses above this range are related to a response *d > 1.0*:

$$d_1(mass) = (a_m \cdot mass + b_m)^{\alpha} \quad (13)$$

a_m, b_m and α influence the response and its shape

so that $\begin{matrix} d_1(mass_{undesired}) \geq 1.00 \\ d_1(mass_{desired}) = 0.01 \end{matrix}$.

The desired mass was defined by a weight saving relative to the differential reference structures. For simplification in all cases presented here the following conditions were used: $m_{desired}$ = *32 kg* and $m_{undesired}$ = *38 kg*.

3.7.5.2. Stability constraints

The out of plane deformation is investigated along a vertical path defined by nodes at the frame-skin intersection. For the integral, innovative structure a path along the frame respectively the window frame is chosen. The influence of possible inclination of the window is avoided by using an interpolation element (MD Nastran® RBE3) between both sides of the window frame (shown in FIG 6).

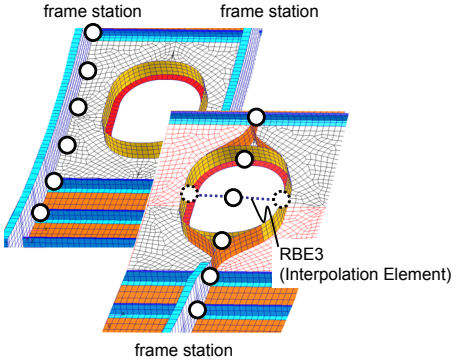

FIG 6. control points for investigation of deformation shape and amplitude; (left: reference structure, right: integral structure)

The application of displacement boundary conditions causes the local model to deform and to perform a rigid body motion in space. The rigid body motion is canceled out by performing two consecutive analyses. A nonlinear simulation of the structure and a linear simulation of the same structure with artificially high stiffness properties in all skin regions is performed. The artificially stiff structure undergoes the same rigid body motion but exhibits almost no other deformations.

The resulting deformation difference is a measure for the amount of nonlinear effects. The deformation difference d_i is calculated for all *n* nodes along the prescribed path. Only the maximum displacement d_{max_disp} is used in the following.

$$d_i^2 = (u_{nl,i} - u_{l,i})^2 + (v_{nl,i} - v_{l,i})^2 + (w_{nl,i} - w_{l,i})^2 \quad (14)$$

$$d_{max\_disp} = \max(d_i) \quad for\ i = 1,2,...n \quad (15)$$

with

u_{nl}, u_l nonlinear and linear displacement in x-direction
v_{nl}, v_l nonlinear and linear displacement in y-direction
w_{nl}, w_l nonlinear and linear displacement in z-direction

The least-square-sum, referred to as $d_{similarity}$, is calculated by

$$d_{similarity} = \sum_{i=1}^{n} d_i^2 \quad (16)$$

and used as a measure for the deformation shapes along the investigated path. These two indicators (d_{max_disp} and $d_{similarity}$) are used for stability evaluation of the designs. The corresponding design responses d_2 and d_3 are again created by the use of an exponential mapping function

$$\begin{matrix} d_2(d_{max\_disp}) = (a_{md} \cdot d_{max\_disp} + b_{md})^{\alpha} \\ d_3(d_{similarity}) = (a_{sd} \cdot d_{similarity} + b_{sd})^{\alpha} \end{matrix} \quad (17)$$

with the coefficients a_{md}, a_{sd}, b_{md}, b_{sd} and α to calibrate the function.

The states used for calibration were defined by the desired state with 1.5 x maximum deflection and the undesired state at 2.5 x maximum deflection of the reference structure. This somehow weaker design constraint was introduced to account for the lower stiffness of the integral structure. The (least-square-sum) similarity criterion allowed larger deformations as well.

Forward and aft reference structures exhibited different deformations (d_{max_disp} and $d_{similarity}$, as shown in TAB 3). Therefore different constraints are accounted for during the optimization of the forward and aft fuselage panels.

3.7.5.3. Fatigue Crack Constraint

The fatigue crack performance of the structure was related to the number of bearable load cycles until the crack reached the next stiffener at a total length of 250 mm.

The mapping function is an exponential relation defined by

$$d_4(N) = (a_{SIF} \cdot N + b_{SIF})^{\alpha} \quad (18)$$

The factors a_{SIF} and b_{SIF} calibrate the function to the desired optimization goals. *N* denotes the number of load cycles.

Cracks in integral structures are more precarious than in differential structures. A significant decrease in the crack growth rate was required by demanding more than *twice as many load cycles* as for the reference structure of the aft fuselage panel. The crack scenario under investigation was based on an initial 20 mm crack (window frame and window rest already broken, detectable by visual inspection) located in the middle of the upper window edge corner. The crack was assumed to grow without deflecting in radial direction (45 degree relative to the horizontal plane).

For simplification purposes all separate optimization runs have used the same constraints demanding for $N_{desired}$ = *15000 cycles* (and avoiding $N_{undesired} \leq$ *10000 cycles*), so that

$$d_4\left(N_{undesired}\right) = 1.00 \qquad d_4\left(N_{desired}\right) = 0.10 \tag{19}$$

3.7.5.4. Failure/Residual Strength Constraint

The failure of the structure was evaluated by calculation of the stress intensity factor for the 2Δp load case of an almost fully torn integral structure (~90 % maximum crack length, crack scenario as described in section 3.7.5.3).

A step function with smooth transition between best (*d = 0.01*) and worst design response (*d = 1.0*) levels was used, described by the following relationships:

$$d_5(K) = \frac{1}{1 + e^{-\lambda \cdot (K/K_C - \Delta)}} \tag{20}$$

with

$$\lambda = \frac{1}{C_{feas}} \left\{ \ln\left(\frac{1}{D_{limit}} - 1\right) - \ln\left(\frac{1}{D_{feas}} - 1\right) \right\} \tag{21}$$

and

$$\Delta = \frac{1}{\lambda} \ln\left(\frac{1}{D_{limit}} - 1\right) + 1 \tag{22}$$

In all cases where $K(a_{max}) < K_c$ (cp. section 2.1 about the fatigue model) the lowest fitness of 0.01 was contributed to the overall fitness function. For values of $K(a_{max}) \geq K_c$ a fitness from 0.5 up to a maximum of 1.0 was assigned.

The shape of the step function is influenced by shape constants D_{feas}, C_{feas}, C_{limit} and D_{limit}. These values have been set to D_{feas} = *0.5*, C_{feas} = *0.1*, C_{limit} = *1.0* and D_{limit} = *0.01* (cp. [2]).

The residual strength was sufficient if the stress intensity *K* remained below K_C (K_C = *2473 N/mm$^{3/2}$*).

3.7.6. Design Objective

The design objective is the minimization of the objective function *F(X)*. Due to the inclusion of design constraints in the objective function the optimization tries to find a solution that features the best trade-off between all included criteria. As a consequence different combinations of design responses can lead to the same overall fitness.

4. RESULTS OF THE OPTIMIZATION

The optimization has been performed for the forward and the rear window panel in separate optimization tasks. Each task used similar settings with a population size μ = 15 and a number of 80 offspring per generation each with a maximum life span of κ = 5. The evolution was performed over 20 generations. The total number of investigated designs reached more than 1500 so that the relevant number of finite element analyses exceeded more than 10000 (in total > 400 CPU hours for each optimization run on an AMD Opteron64®, 2.2GHz, 2 GB RAM Linux system, performed on 8 cluster nodes in ~2 days).

4.1. Optimized Integral Aft fuselage panel

The optimized design for the integral fuselage panel located in the aft of the fuselage is characterized by the following combination of design variables given in TAB 5.

vertical stiffener	diagonal stiffener	horizontal stiffener	h_{frame} /(mm)	$h_{central\ control\ point}$ /(mm)	$h_{central\ intermed.\ point}$ /(mm)
no	yes	yes	42.1	60.0	60.0

TAB 5. optimized design variables (aft fuselage panel)

The optimization of the aft fuselage panel improved relative to the initial integral starting point in all criteria (TAB 6). In comparison with the differential reference structure the benefit of the optimization seems to be smaller: The crack growth improved significantly but still did not meet the desired performance of 15000 load cycles. The same can be observed for the structure's mass that remained above the desired level of 32 kg. However, the displacement design constraints, as a measure for the stability of the structure, decreased and almost met the design goal.

Model	mass /(kg)	N (a_{max}) /(cycles)	$d_{maxdisp}$ /(mm)	$d_{similarity}$ /(mm)	$K_{res\ strength}$ /(Nmm$^{3/2}$)
Integral Optim.	34.17	12400	1.67	5.71	2390
In comparison with differential structure:					
	(d) 6%	(i) 58%	(d) 96%	(d) 56%	(d)
In comparison with integral initial structure:					
	(i) 0.4%	(i) 65%	(i) 17%	(i) 39%	(i)

(d) deterioration of the optimized solution vs. reference
(i) improvement of the optimized solution vs. reference

TAB 6. performance changes (aft fuselage panel)

The success of the optimization procedure and the evolution of the designs can be investigated by examination of the average fitness of the population. FIG 7 depicts the average fitness of all offspring over the generations. The addends to the overall fitness are shown by separate curves: Over the first generations the average fitness of the displacement criteria improved significantly. Meanwhile the average structural mass and the average fitness for the fatigue crack and residual strength criteria increased.

The reason for this behavior is given by the different influence of the design variables on the structure's behavior. The existence of stiffeners leads to significant improvement of the displacement behavior but increased the struc-

ture's mass. This trade-off remains in the population's gene pool and creates a kind of Pareto optimal design, which features either a low weight or a favorable fatigue crack and deformation performance.

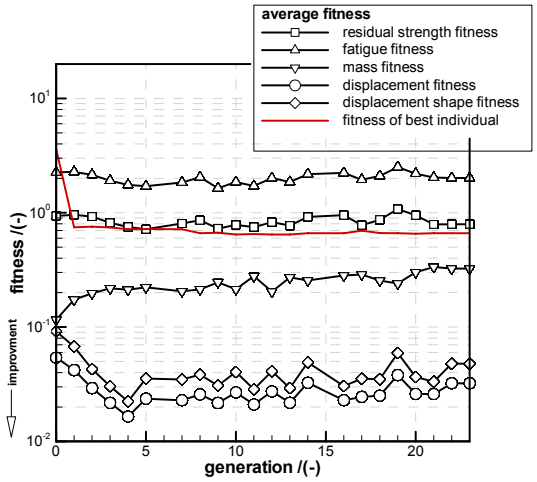

FIG 7. history of design variables, aft fuselage panel

The fitness of the best individual of each generation is plotted as well in FIG 7. Starting with a poor fitness of ~4 in the first generation a fast improvement is achieved already after a few generations. The final fitness does not meet the defined optimization goal and remains at ~0.644 ($\leq$ 0.1 desired)[3].

4.2. Optimized Integral Forward fuselage panel

The best obtained combination of design variables for the integral panel in the forward part of the fuselage is given in TAB 7.

vertical stiffener	diagonal stiffener	horizontal stiffener	h_{frame} /(mm)	$h_{central\ control\ point}$ /(mm)	$h_{central\ intermed.\ point}$ /(mm)
yes	yes	no	30.0	29.2	60.0

TAB 7. optimized design variables (forw. fuselage panel)

The result is significantly different from the result for the aft fuselage section due to the different geometry (e.g frame dimensions) and especially due to the different loading conditions. Relative to the initial integral reference an improvement is achieved with respect to all investigated criteria. But again, the performance of the differential reference structure is in some disciplines still better, especially in cases where bending stiffness is required (stability).

Model	mass /(kg)	N (a_{max}) /(cycles)	$d_{maxdisp}$ /(mm)	$d_{similarity}$ /(mm)	$K_{res\ strength}$ /(Nmm$^{3/2}$)
Integral Optim.	34.96	64900	3.08	19.9	2480
In comparison with differential structure:					
	(i) 1.4%	(i) 115%	(d) 105%	(d)100%	(d)
In comparison with integral initial structure:					
	(i) 2.9%	(i) 34%	(i) 14%	(i) 21%	(i)
(d) deterioration of the optimized solution vs. reference (i) improvement of the optimized solution vs. reference					

TAB 8. performance changes (forward fuselage panel)

The evolution of the population during the design optimization is similar to the results given in section 4.1: the gene pool of the population remains for a long time very non-uniform due to different possibilities to combine design variables and to achieve a comparable design.

The final design for the forward fuselage panel features a total fitness of 1.148 which indicates that the optimization goals have not been met in every discipline[4]. Although the mass has decreased (relative to the initial integral structure and as well relative to the differential reference) the design response related to the mass still assigns a value of 0.356 to the mass of 35 kg because the goal (32 kg) has not been met. The displacement based criteria, as an indicator for the global buckling sensitivity, remained above the prescribed limit, too. Probably the definition of the design task (combination of desired weight and desired performance) demanded for an infeasible design.

4.3. Benefits of Integral Structures

The integral structures under investigation showed a performance that is compatible with the self-defined reference. To find an applicable design more elaborate investigations are needed. Especially the investigation of the stability performance is challenging and might not be suitable for a comparison between designs that are in principle different.

Nevertheless the freedom in design can be used to align the structures topology with the occurring loading situation. In combination with reduction in manufacturing costs a benefit is reasonable.

5. CHALLENGES FOR FUTURE DESIGN INVESTIGATIONS – DATON

The fatigue crack examples given above have all been stopped at a scenario, where the crack-tip reached the vicinity of the next stiffener, but did not pass it. Especially this scenario is obviously of major importance for the assessment of the damage tolerance capacity of the integrally stiffened structure compared with the differential one. The problem is that there will not be one solution for integrally stiffened structures compared with differential ones, but instead a set of solutions, depending mainly on the residual stresses introduced by the manufacturing process, i.e. HPC, FSW and LBW. On top, the process of cracking of an integrally stiffened structure is a relatively complex one and needs more, mainly 3D-modelling. On the other hand, optimization procedures, as shown here, need fast, but reliable methods, which is also a task.

The project DaToN of the 6th framework program of the European Commission has the aim to investigate the crack propagation and partly also the residual strength problem of integrally stiffened structures, manufactured by the three methods named above. The project started on April 2005 and will be finalised in fall 2008. A consortium of initially 15 partners has been built. The partners are: Airbus Deutschland, EADS IW (both France and Germany), IAI, ASM Technology, DLR, NLR, FOI, University of Patras, University of Pisa, University of Sheffield Hallam,

[3] d_1 = 2.61e-1, d_2 = 8.5e-3, d_3 = 2.53e-3, d_4 = 3.72e-1, d_5 = 4.7e-6

[4] d_1 = 3.56e-1, d_2 = 4.04e-1, d_3 = 3.61e-1, d_4 = 0.0, d_5 = 2.73e-2

University of Brno, Imperial College and as coordinator the institute of the authors. The work comprises both, theoretical methods and experiments, as well as a verification task and a task which tries to develop guidelines for the industrial application. Three different materials have been chosen, building a matrix with 9 different combinations of manufacturing methods and materials.

Meanwhile a relatively good agreement in K-solutions is found by several methods used by the partners. It can be shown that residual stresses and material data are of major importance for a good prediction of the crack growth.

6. CONCLUSION

The investigation of integral airframe structures requires special attention to cover the relevant design drivers. In order to fully explore the freedom in design obtained by alternative manufacturing techniques an optimization procedure with multiple design constraints has been adopted. Different load cases corresponding to the design criteria are considered.

The optimization required a significant amount of computation time and leads to a solution that has improved relative to an initial, integral reference and as well to a differential reference in some criteria. To fully identify the potential of integral structures further numerical investigations are necessary. These should include on the one hand an improvement of the methodology to calculate the fatigue crack performance (as being done in DaToN) and on the other hand a closer assessment of the applied stability criteria.

However, the first results are promising and might help in the development of (cost-efficient) metallic alternatives to composite designs.

REFERENCES

[1] Bäck, T., Hammel, U., Schwefel, H.-P. Evolutionary Computation: Comments on the History and Current State, IEEE Trans. Evolutionary Computation, Vol.1, pp. 3-17, Apr. 1997.
[2] Gieger, M., Ermanni, P. Development of CFRP racing motorcycle rims using a heuristic evolutionary approach, Structural and Multidisciplinary Optimization, Vol. 20, 54-65 (2005).
[3] Hansen, L. U., Heinze, W., Horst, P. Representation of Structural Solutions in Blended Wing Body Preliminary Design. Proceedings of the 25th ICAS-Congress in Hamburg, 2006.
[4] Hansen, L. U., Horst, P. Structural Concept Optimization in Preliminary Aircraft Design, 7th World Congress on Structural and Multidisciplinary Optimization WCSMO, Korea, May 2007.
[5] Hansen, L.U., Häusler, S.M., Horst, P. Evolutionary Multicriteria Design Optimization of Integrally Stiffened Airframe Structures, submitted to the Journal of Aircraft, under review since March 2007.
[6] Häusler, S.M., Reim, A.D., Horst, P. Fatigue Crack Growth – A Challenge for New Integrally Stiffened Aircraft Structures, Proceedings of the 24th ICAF Symposium, Naples 16-18 May 2007.
[7] HSB, Abschätzung der Rissfortschrittsraten für metallische Werkstoffe mit Hilfe der Forman-Gleichung, Blatt 63205-01, Handbuch Struktur Berechnung, 1989.
[8] Krueger, R. Virtual Crack Closure Technique: History, approach, and applications, Appl. Mech. Rev, Vol.57, No. 2, March 2004.
[9] Munroe, J., Wilkins, K., Gruber, M. Integral Airframe Structures (IAS) — Validated Feasibility Study of Integrally Stiffened Metallic Fuselage Panels for Reducing Manufacturing Costs, NASA/CR-2000-209337, 2000.
[10] Österheld, C. Physikalisch begründete Analyseverfahren im integrierten multidisziplinären Flugzeugvorentwurf, Dissertation TU Braunschweig, ZLR Forschungsbericht 2003-06, 2003.
[11] Pacchione, M., Telgkamp, J. Challenges of the metallic fuselage, Proc. of the 25th International Congress on Aeronautical Sciences ICAS 2006, Hamburg 2006.
[12] Pettit, R.G., Wang, J.J., Toh, C. Validated feasibility study of integrally stiffened metallic fuselage panels for reduced manufacturing costs, Technical Report NASA/CR-2000-209342, 2000.
[13] Schwefel, H.-P., Rudolph, G., Bäck, T. Contemporary Evolution Strategies. In European Conference on Artificial Life, pages 893-907, 1995.
[14] Schwefel, H.-P. Evolution and Optimum seeking, Wiley-Interscience, John Wiley & Sons Inc., New York, 1995.

APPENDIX

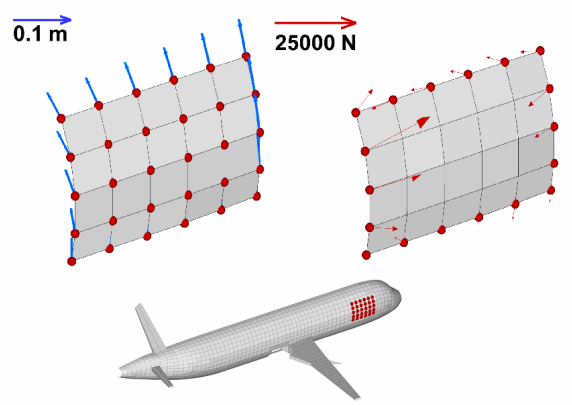

FIG 8. displacement (left) and force (right) boundary conditions, bending load case, forward fuselage

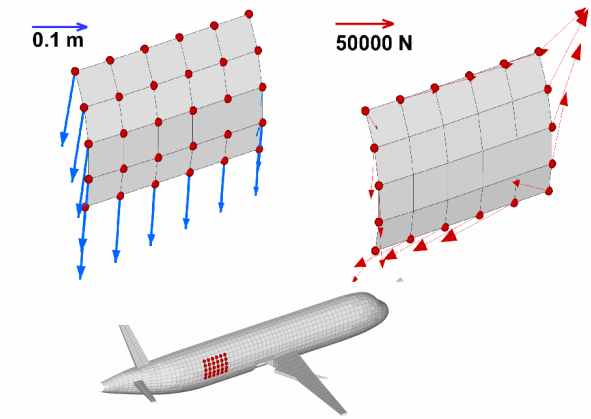

FIG 9. displacement (left) and force (right) boundary conditions, bending load case (aft fuselage)